

Charge spectrometry with a strongly coupled superconducting single-electron transistor

C. P. Heij, P. Hadley, and J. E. Mooij
Applied Physics and DIMES, Delft University of Technology
Lorentzweg 1, 2628 CJ Delft, The Netherlands
(November 13, 2018)

We have used a superconducting single-electron transistor as a DC-electrometer that is strongly coupled to the metal island of another transistor. With this set-up, it is possible to directly measure the charge distribution on this island. The strong capacitive coupling was achieved by a multilayer fabrication technique that allowed us to make the coupling capacitance bigger than the junction capacitances. Simulations of this system were done using orthodox theory of single-electron tunnelling and showed excellent agreement with the measurements.

A single-electron transistor can make extremely sensitive charge measurements with a resolution of about $10^{-5} e/\sqrt{\text{Hz}}$.¹⁻³ In principle, this sensitivity is sufficient to measure the charging and discharging of a small conductor as current flows through that conductor. A single-electron transistor would be able to register the tunnelling of individual electrons tunnel onto the conductor from one lead and off the conductor to another lead for currents up to a few picoampères. In practice, the high output impedance of a single-electron transistor makes this measurement very difficult. If the charge on the conductor as a function of time could be measured, then it would be possible to determine the occupation probabilities of the various charge states. In charge state $\langle 0 \rangle$ the conductor is neutrally charged, in charge state $\langle 1 \rangle$ the conductor has an excess charge of one electron, and so forth. The charge state occupation probabilities play a central role in the theory of single-electron tunnelling^{4,5} but are typically not directly accessible experimentally. Here we report on an experiment where a superconducting single-electron transistor (SSET) was used to directly measure the charge state occupation probabilities on the island of another nearby SSET.

An essential feature of this experiment was that the measurement SSET (the electrometer) was strongly coupled to the island where the current was flowing through. Strong coupling means that the coupling capacitance was comparable to the total capacitance of the nearby island. When one electron was added to this island, about $e/4$ of charge was induced on the coupling capacitor. The electrometer was biased at a small voltage and its tuning gate was used to scan the charge on the neighboring island. These gate traces directly reflect the charge distribution on this island. The measurements are consistent with orthodox theory and they show that a strongly coupled SSET can be used to directly measure the charge distribution.

I. EXPERIMENT

A schematic of the device is shown in Fig. 1a. The device was fabricated in three layers. The junctions were fabricated using standard shadow evaporation of aluminum. SSET1 has a planar gate capacitor C_{g1} while the gate capacitor C_{g2} is defined as a parallel plate capacitor. Details of the fabrication of a similar device were described elsewhere.⁶ Figure 1b shows a SEM picture of the device. The two square islands of the SSETs are coupled via an underlying dumbbell shaped coupling capacitor. The total effective capacitance between the two islands is called C_m . Both SSETs were biased asymmetrically, connected to a voltage source at one side and grounded at the other side. The device was measured in a dilution refrigerator with a base temperature of 10 mK. The leads were equipped with π -filters at room temperature and standard copper-powder filters at base temperature. The effective electron temperature, 25 mK, was measured in the normal state by fitting experimentally obtained Coulomb peaks. All further measurements were done in the superconducting state, the superconducting gap being $\Delta = 200 \mu\text{eV}$.

Throughout the measurements, the voltage bias of the electrometer was kept constant at $V_{b1} = 805 \mu\text{V}$, just above $4\Delta/e$. The current through the electrometer I_1 was measured as a function of the gate voltage V_{g1} and the bias voltage V_{b2} of the SSET2. The gate voltage V_{g2} was kept constant. Figure 2a shows typical Coulomb oscillations of the current through the electrometer. The gate of the electrometer was swept while SSET2 was biased at 800 μV , the current I_2 being negligibly small. Figure 2b shows the same Coulomb trace when $V_{b2} = 890 \mu\text{V}$, above the quasiparticle threshold of SSET2. Surprisingly, the Coulomb peak is split into two peaks, while at even higher bias ($V_{b2} = 1090 \mu\text{V}$) it is split into three. As we will explain below, each extra peak can be attributed to the presence of an extra electron on the second island.

When $V_{b2} = 800 \mu\text{V}$, the current through SSET2 is still negligibly small and the occupation probability of charge state $\langle 0 \rangle$ on island 2 is nearly 1. When V_{b2} is higher than the threshold voltage, a quasiparticle current I_2 will start to flow and the charge n_2 on the island 2 will switch between $\langle 0 \rangle$ and $\langle 1 \rangle$. The presence of an extra electron on island 2 will induce a fraction of an electron on coupling capacitor C_m . By writing down the total charge on both islands as a function of the capacitances and the island potentials, one can show that this fraction is $C_m/C_{\Sigma 2}$, where $C_{\Sigma 2}$ is the sum of all capacitors connected directly to island 2. Table I gives the capacitance and resistance values of all the circuit elements. With this table, we can calculate that the charge induced on capacitor C_m is $0.27 e$. This results in the extra Coulomb peak (labelled $\langle 1 \rangle$) shifted $-e/C_{g1} * 0.27 = -1.04 \text{ mV}$ with respect to the peak labelled $\langle 0 \rangle$ in Fig. 2b. When V_{b2} is increased even more, charge state $\langle 2 \rangle$ is also populated on island 2 and three peaks appear (Fig. 2c). Figure 3 shows the Coulomb traces of the electrometer current I_1 in grayscale versus the bias V_{b2} . One can clearly see that consecutive charge states become populated with increasing V_{b2} . The average bias voltage difference between successive charge states on island 2 is $2E_{C2}/e$, where E_{C2} is the charging energy of island 2. The charge state $\langle 4 \rangle$ becomes populated at $V_{b2} = 1180 \mu\text{V}$ and induces $1.08 e$ on island 1. The corresponding peak in the Coulomb trace of the electrometer overlaps with the next set of Coulomb peaks, limiting the number of observable charge states to four with these circuit parameters.

By measuring Coulomb oscillations, the electrometer can be used to directly resolve the average population of charge states on a nearby island, even though the charge on this island changes on a nanosecond timescale. At Coulomb peak $\langle j \rangle$, current can only flow through the electrometer when the island 2 is in charge state $\langle j \rangle$. The fraction of the time that island 2 spends in charge state $\langle j \rangle$ is equal to the relative peak height defined by,

$$p_i = \frac{I_{p,i}}{\sum_j I_{p,j}}, \quad (1)$$

where $I_{p,j}$ is the peak height of the Coulomb peak corresponding to the charge state $\langle j \rangle$ on island 2. Simulations confirm that the height of the individual peaks reflects the exact population of the corresponding charge state.

The relative peak heights of the Coulomb traces in Fig. 2b,c are calculated and shown in column I of Table II. They closely match the occupation of the various charge states as calculated in the simulations for identical bias conditions, shown in column II. Also, for bias conditions other than $V_{b2} = 890 \mu\text{V}$ and $1020 \mu\text{V}$, the simulated relative peak heights closely match the experimental ones. This shows that a strongly coupled SSET can be used to quantitatively measure the charge *distribution* on a nearby object.

II. SIMULATIONS

The current through both SSETs was calculated using a master equation analysis. By solving the master equation we can calculate the occupation probabilities of the various charge states. The master equation for this two island system is,

$$\frac{\partial P_{ij}}{\partial t} = \sum_{kl \neq ij} (P_{kl} \Gamma_{kl \rightarrow ij} - P_{ij} \Gamma_{ij \rightarrow kl}), \quad (2)$$

$$\sum_{ij} P_{ij} = 1, \quad (3)$$

where P_{ij} is the probability that the system has i excess electrons on island 1 and j excess electrons on island 2. Γ denotes the transition rate between different charge states. In the stationary state, P_{ij} does not change and the left hand side of equation 2 is zero. The first term on the right describes the population of charge state ij from charge state kl while the second term describes the depopulation of charge state ij to charge state kl . We neglect co-tunnelling processes and Γ only is non-zero when either $i = k \pm 1$ or $j = l \pm 1$. Furthermore we only take into account a maximum of five charge states per island.

The superconducting tunnel rates Γ were then determined with Fermi's Golden Rule using the superconducting density of states and the free energy difference ΔF of a tunnelling event.^{7,8} ΔF is the sum of the change in electrostatic energy plus the work done by the voltage sources. The total electrostatic energy of the system can be written as:

$$E(n_1, n_2) = E_{C1}(n_{01} + n_1)^2 + E_{C2}(n_{02} + n_2)^2 + E_m(n_{01} + n_1)(n_{02} + n_2), \quad (4)$$

$$E_{C1} = \frac{e^2 C_{2\Sigma}}{2(C_{\Sigma 1} C_{\Sigma 2} - C_m^2)} = 95 \mu\text{eV}, \quad (5)$$

$$E_{C2} = \frac{e^2 C_{1\Sigma}}{2(C_{\Sigma1} C_{\Sigma2} - C_m^2)} = 53 \mu\text{eV}, \quad (6)$$

$$E_m = \frac{e^2 C_m}{C_{\Sigma1} C_{\Sigma2} - C_m^2} = 51 \mu\text{eV}, \quad (7)$$

where n_{01} and n_{02} are the normalized charges induced on the islands by the voltage sources, n_1 and n_2 are the excess number of electrons on the islands and $C_{\Sigma1}$ and $C_{\Sigma2}$ are the sum of all capacitors directly connected to the respective islands. The electrostatic energy has three contributions, the charging energies of the separate SSETs (equations 5 and 6) and the coupling energy E_m , which describes the electrostatic interaction between both SSETs. When equations 2 and 3 are solved for P_{ij} , the total current I_1 can be calculated with P_{ij} and the tunnel rates.

In Fig. 4 the current through the electrometer has been calculated for the same bias conditions as Fig. 2. One can clearly see the extra Coulomb peaks appear when the bias voltage V_{b2} is increased. The absolute peak height of the experiments is about 60% of the peak height in the simulations. This can be accounted for by the rounding of the superconducting gap. Instead of the discontinuous jump in quasiparticle current through a superconducting junction at $2\Delta/e$, in real experiments, the current increases with a non-zero slope. In these experiments, the differential resistance in this regime is about 5% of the high bias junction resistance. For a bias voltage of $V_{b1} = 805 \mu\text{V}$, only $5 \mu\text{V}$ above $4\Delta/e$, this has two consequences. First, the Coulomb peaks have a more triangular form as can be seen in Fig. 2, second, the Coulomb peak height is smaller than in the simulations where the rounding has not been taken into account. Simulations where the rounding of the gap was taken into account with a simple model showed that the rounding of the gap does not change the relative height of the peaks, it merely decreases the overall current.

For the simulated Coulomb traces of Fig. 4, the relative peak heights as specified by Equation 1 are given in Table II. The experiments closely match the simulated values. The relative peak heights in simulations are slightly different though from the occupation of the charge states on island 2 when the electrometer is switched "off" ($V_{b2} = 800 \mu\text{V}$). Column three of Table II shows the undisturbed occupancies of the three charge states as determined from the population matrix P_{ij} . As can be seen from Table II, the bias of the electrometer has a small back action on the occupation of charge states on island 2. For the bias range of Fig. 5, it can be shown that the back action of this electrometer changes the occupancies of the various charge states by a maximum of 5%.

Figure 5 is the simulated equivalent of Fig. 3. The extra peaks appear in Fig. 5 at exactly the same bias conditions as in Fig. 3, demonstrating the close agreement between experiments and simulations. Another feature that clearly shows up in the simulations as well as the measurements is the existence of a current plateau in between the neighboring Coulomb peaks. Under these bias conditions, the electron-tunnelling through both SSETs is correlated. This effect has been described before in coupled 1D arrays of tunnel junctions.^{9,10} The details of this effect will be discussed below.

III. DISCUSSION

The ability to determine the position and the height of the extra Coulomb peaks gives constraints on the bias conditions. In general, the width of the peaks has to be smaller than the separation between adjacent peaks. In the superconducting state the width of Coulomb peaks is almost independent of temperature for $k_B T < 0.5\Delta$ and depends linearly on the applied bias. This constraint can be rewritten as:

$$eV_{b1} - 4\Delta < E_m. \quad (8)$$

This simply states that the energy associated with the voltage bias has to be smaller than the coupling energy. Because of the quasiparticle threshold at $4\Delta/e$, this constraints the bias voltage to $800 \mu\text{V} < V_{b1} < 851 \mu\text{V}$ for this sample. The quasiparticle rate is almost independent of the bias in this bias window and simulations indicate that the back action of the electrometer is also constant. If we take into account the rounding of the gap and the experimental current noise, $V_{b2} = 805 \mu\text{V}$ is about the optimal bias voltage, combining an acceptable signal to noise ratio with a reasonably small width of the Coulomb peaks. With the current sample parameters, we are limited to the observation of a maximum of four charge states on the neighboring island. We estimate that it is feasible to observe at least seven different charge states, when the coupling capacitance is lowered to 190 aF, while keeping the other sample parameters constant.

Both Fig. 2 and 4 clearly show the existence of a current plateau in between the accompanying Coulomb peaks. In order to be able to measure the relative peak heights, this plateau current should not exceed the Coulomb peak current and therefore its mechanism should be understood. The mechanism can be most easily explained when the

number of occupied electron states on island 2 is limited to two and under the assumption that the tunnel rates in SSET1 are much larger than those in SSET2. Figure 6a schematically displays the quasiparticle thresholds for SSET1. The position of the dots denotes the effective background charge when the charge state of island 2 is $\langle 0 \rangle$ (right dot) and $\langle 1 \rangle$ (left dot). The position of the dots relative to each other is fixed. The bias voltage V_{b1} and hence the dots lie just above $4\Delta/e$. With the gate voltage V_{g1} the position of both dots can be shifted along the Q_{01} axis. If the gate voltage positions one of the two dots above both quasiparticle thresholds α and β this leads to current in the form of a Coulomb peak. If the dots are positioned as depicted in Fig. 6a there is an additional mechanism that will carry current.

The charge states with the lowest energy are now $\langle 10 \rangle$ and $\langle 01 \rangle$. If a current is forced to flow through SSET 2 by biasing it above its quasiparticle threshold, the following current cycle is most probable: If we start with charge state $\langle 00 \rangle$ it is only favorable for electrons to tunnel onto islands 1 or 2 via the top junctions. Because we assume that the tunnel rates in SSET1 are much larger than those in SSET2, an electron will most probably tunnel through junction j1 first, as shown in Fig. 6b. Now the system is in the charge state $\langle 10 \rangle$ which is stable for electron tunnelling in SSET1. After some time the bias voltage V_{b2} forces an electron on island 2 and the system is in state $\langle 11 \rangle$. As can be seen in Fig. 6c this state decays to $\langle 01 \rangle$ through junction j2, again assuming the tunnel rates are much higher in SSET1. This charge state is also stable for electron tunnelling in SSET1. The cycle is completed when the electron is forced off island 2 and the system is back in charge state $\langle 00 \rangle$. The cycle of one electron tunnelling through SSET2 has transported another electron through SSET1 making $I_1 = I_2$. This cycle is possible for all gate voltages where both the position of $n_2 = \langle 1 \rangle$ lies below quasiparticle threshold α and position of $n_2 = \langle 0 \rangle$ lies below quasiparticle threshold β . This gives rise to a current plateau exactly in between the Coulomb peaks attributed to the both charge states.

In this sample, the resistances of SSET1 and SSET2 and hence the tunnel rates differ by only a factor of two. This means that cycles can be missed, for example if state $\langle 00 \rangle$ decays to $\langle 01 \rangle$, the system is forced to $\langle 00 \rangle$. An electron is transported through SSET2, without giving rise to current in SSET1. The general equation for the relation between I_1 and I_2 can be deduced by analytically solving the master equation under the assumption that only the four charge states $\langle 00 \rangle$, $\langle 10 \rangle$, $\langle 01 \rangle$ and $\langle 11 \rangle$ need to be considered. If we assume that the tunnel rates through junction j1 and j2 are equal and called Γ_1 , as well as those through j3 and j4 are equal and called Γ_2 this yields:

$$I_1 = \frac{\Gamma_1}{\Gamma_1 + 2\Gamma_2} I_2. \quad (9)$$

By deriving the expressions for the Coulomb peak current, it can be shown that the peak currents are always sufficiently larger than the plateau current, making it possible to adequately determine the relative peak heights. When the number of occupied charge states on island 2 is larger than two, the mechanism leading to the current plateaus is similar, but different combinations of charge states might be stable and equation 9 will be modified. Again though, the plateau current is always smaller than the Coulomb peaks adjacent to the particular current plateau.

We also studied the performance of the electrometer in the normal state. In the normal state, however, the Coulomb peaks are very sensitive to thermal fluctuations. The thermal broadening of the Coulomb peaks at 70 mK was enough to merge the adjacent Coulomb peaks, making an accurate determination of the relative peak heights impossible. Additionally, due to a mechanism similar to the one leading to plateau current in the superconducting state, the adjacent Coulomb peaks merged at 30 mK in the normal state, making the normal state operation of this electrometer impractical.

IV. CONCLUSIONS

We have used a SSET to measure the charge distribution on a neighboring island. Both the islands were strongly coupled by a multi-layer technology. The presence of an extra electron on a neighboring island split the Coulomb peaks of the SSET. The relative height of these peaks directly translates to the occupation of the associated charge state. In between the neighboring Coulomb peaks the current is carried by correlated tunnelling of electrons through both SSETs.

V. ACKNOWLEDGEMENTS

We thank K. K. Likharev for illuminating the basic mechanism leading to the current plateau.

-
- ¹ V. A. Krupenin, D. E. Presnov, A. B. Zorin, and J. Niemeyer, *J. Low Temp. Phys.* **118** 287 (2000).
- ² R. J. Schoelkopf, P. Wahlgren, A. A. Kozhevnikov, P. Delsing, and D. E. Prober, *Science* **280** 1238 (1998).
- ³ E. H. Visscher, J. Lindeman, S. M. Verbrugh, P. Hadley, J. E. Mooij, and W. van der Vleuten, *Appl. Phys. Lett* **68** 2014 (1996).
- ⁴ D. V. Averin and K. K. Likharev, in *Mesoscopic Phenomena in Solids*, ed. by B. L. Altshuler, P. A. Lee, and R. A. Webb. Amsterdam: Elsevier 173 (1991).
- ⁵ G. L. Ingold and Yu. V. Nazarov, in *Single Charge Tunneling*, ed. by H. Grabert and M. H. Devoret, New York: Plenum 21-108 (1992).
- ⁶ C. P. Heij, D. C. Dixon, P. Hadley, and J. E. Mooij, *Appl. Phys. Lett.* **74** 1042 (1999).
- ⁷ See for example M. Tinkham, *Introduction to Superconductivity* p. 77 (McGraw-Hill, New York, 1996), second edition.
- ⁸ Using Fermi's golden rule we numerically calculate the superconducting rates assuming the BCS density of states, which is proportional to $\frac{E}{(E^2 - \Delta^2)^{\frac{1}{2}}}$.
- ⁹ D. V. Averin, A. N. Korotkov, and Yu. V. Nazarov, *Phys. Rev. Lett.* **66** 2818 (1991).
- ¹⁰ M. Matters, J. J. Versluys, and J.E. Mooij, *Phys. Rev. Lett.* **78** 2469 (1997).

(a) SSET1 SSET2
 “electrometer”

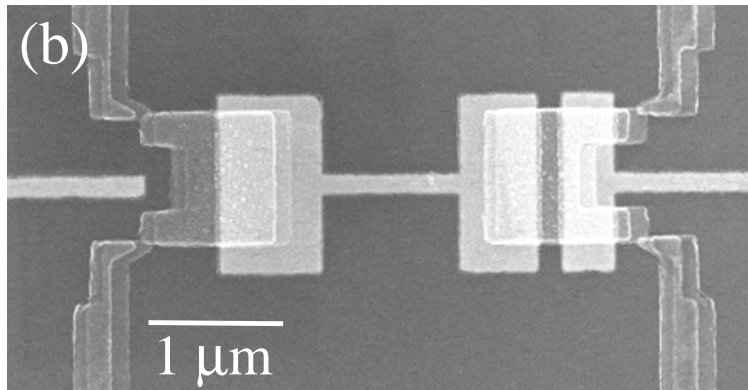
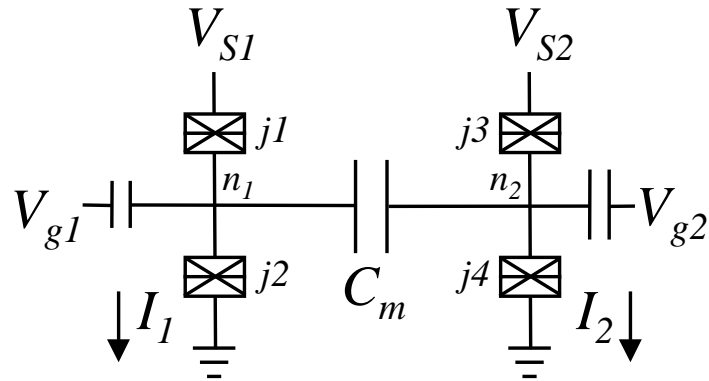


FIG. 1. (a) Schematic of the circuit. The two junctions on the left form the electrometer (SSET1), whose island is coupled capacitively to the island of a nearby SSET (SSET2). (b) Scanning electron microscope picture of the completed device. The light gray layer is fabricated in gold, the aluminum layer shows up as dark grey.

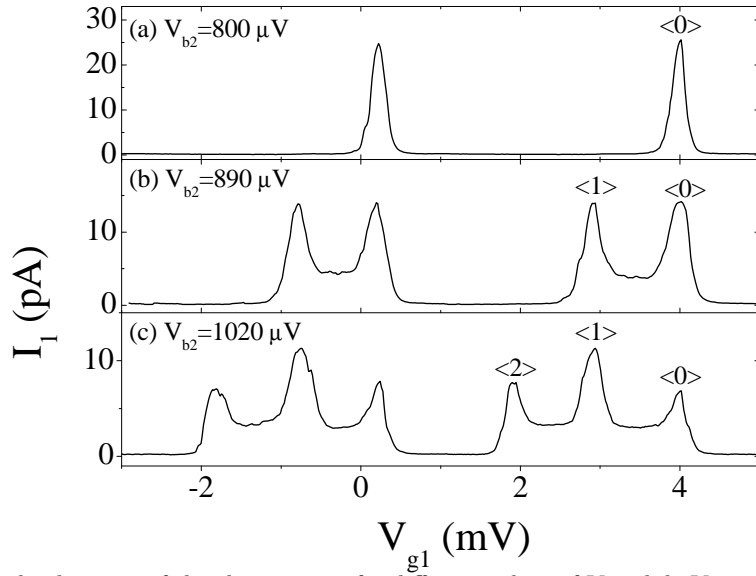


FIG. 2. Experimental Coulomb traces of the electrometer for different values of V_{b2} while $V_{b1} = 5\mu\text{V}$, $V_{g2} = 10\mu\text{V}$ and $T=25\text{ mK}$. The extra peaks Coulomb peaks in (b) and (c) correspond to the presence of extra electrons on island 2.

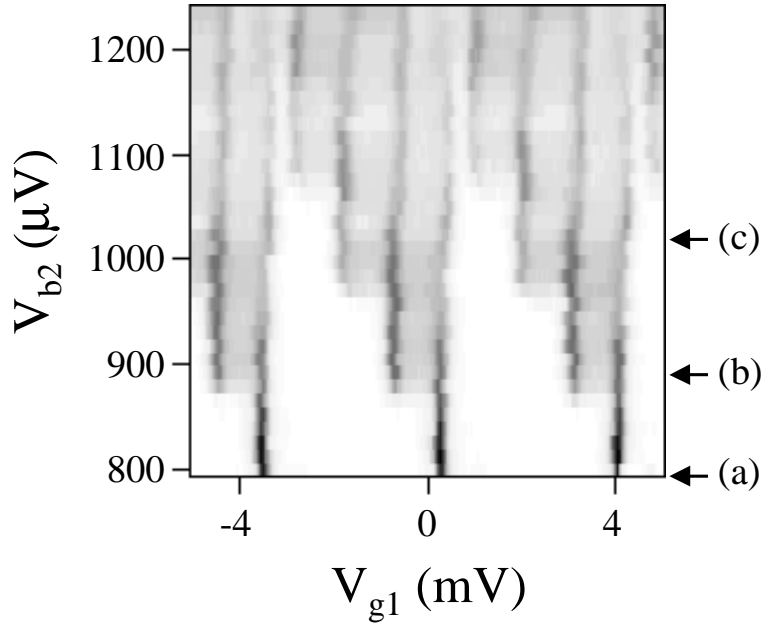


FIG. 3. Electrometer current versus V_{g1} and V_{b2} . White indicates no current, black indicates a maximum current of 25 pA. The arrows indicate the values of V_{b2} where the traces of Fig. 2a-c have been extracted. At $V_{b2} = 1180\mu\text{V}$ the charge state $\langle 4 \rangle$ becomes populated, but the corresponding peak overlaps with the neighboring set of Coulomb peaks.

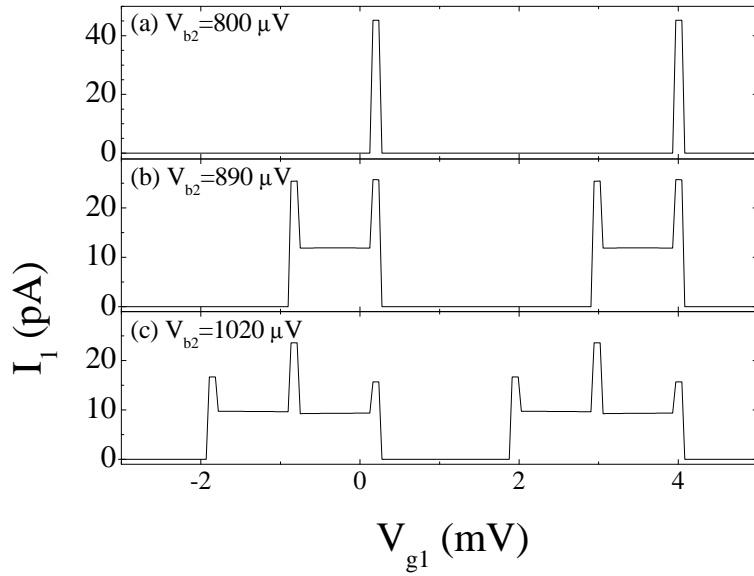


FIG. 4. Simulations of Coulomb traces of the electrometer for different values of V_{b2} . $V_{b1} = 805 \mu\text{V}$, $V_{g2} = 10 \mu\text{V}$ and $T=25 \text{ mK}$.

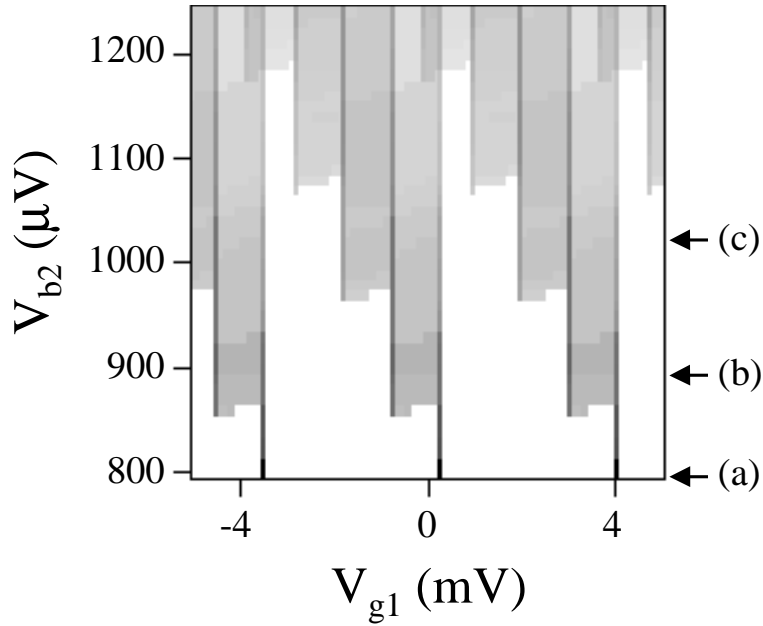


FIG. 5. Simulation of the electrometer current versus V_{g1} and V_{b2} . White indicates no current, black indicates a current of 45 pA. The arrows indicate the values of V_{b2} where the traces of Fig. 4a-c have been extracted.

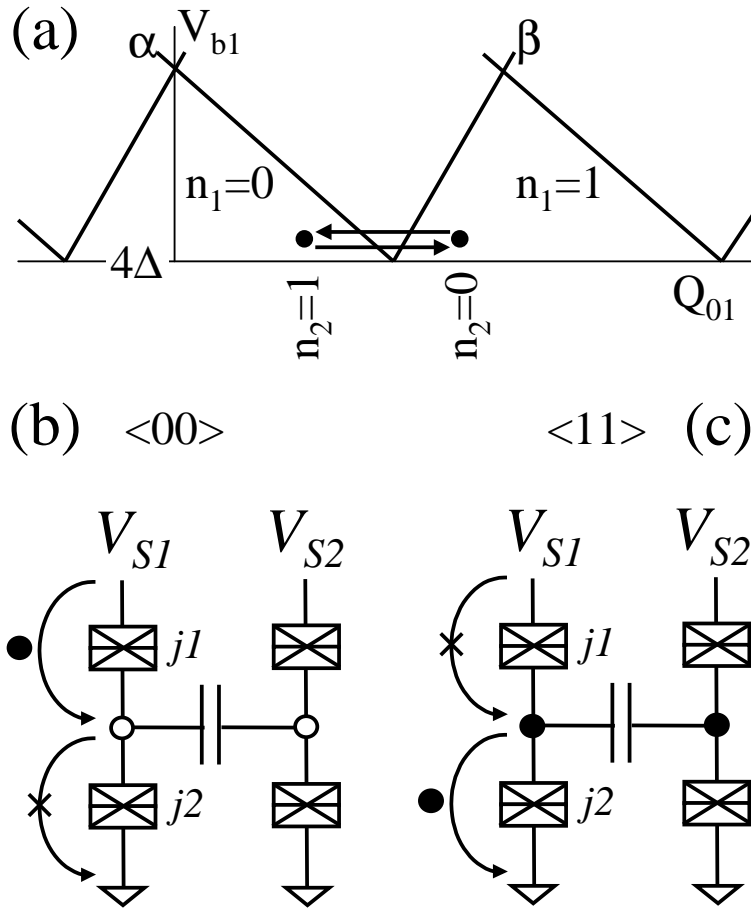


FIG. 6. (a) Schematic of the quasiparticle thresholds of SSET1 above $V_{b1} = 4\Delta/e$, shown as thick lines. The positions of the dots denote the effective background charge induced by the absence or presence of an extra electron on island 2. (b) Visualization of the possible tunnelling events on island 1. When the system is in charge state $\langle 00 \rangle$ it will decay to $\langle 10 \rangle$ by an electron tunnelling through junction $j1$. Electron tunnelling through junction $j2$ is energetically unfavorable, just like electrons tunnelling upward. (c) In a similar way charge state $\langle 11 \rangle$ decays to $\langle 01 \rangle$.

	j1	j2	j3	j4	C_{g1}	C_{g2}	C_m	$C_{\Sigma 1}$	$C_{\Sigma 2}$
C (aF)	135	350	160	400	42	640	450	977	1650
R (M Ω)	3.5	3.5	6.5	6.5	∞	∞	∞	-	-

TABLE I. Capacitance and resistance values for the circuit parameters as calculated from the stability diagrams and current-voltage characteristics of both SSETs.

	I. experiments			II. simulations			III. SSET1 'off'		
V_{b2} (μ V)	p_0	p_1	p_2	p_0	p_1	p_2	p_0	p_1	p_2
890	0.50	0.50	0	0.50	0.50	0	0.50	0.50	0
1020	0.28	0.43	0.29	0.28	0.42	0.30	0.29	0.40	0.31

TABLE II. The population of first three charge states on island 2, as calculated from the peak heights in the experiments (Fig. 2) and the simulations (Fig. 4). The undisturbed population is determined by a calculation of the population matrix P_{ij} of equation 2 when the electrometer is switched off ($V_{b1} = 800\mu$ V).